Adsorption geometry and core excitation spectra of three phenylpropene isomers on Cu(111)

C. Kolczewski[a)]
Fritz-Haber-Institut der Max-Planck-Gesellschaft, Faradayweg 4-6, 14195 Berlin, Germany

F. J. Williams, R. L. Cropley, O. P. H. Vaughan, A. J. Urquhart,
M. S. Tikhov, and R. M. Lambert
Department of Chemistry, University of Cambridge, Cambridge CB2 1EW, United Kingdom

K. Hermann
Fritz-Haber-Institut der Max-Planck-Gesellschaft, Faradayweg 4-6, 14195 Berlin, Germany

Theoretical C $1s$ near edge x-ray absorption fine structure (NEXAFS) spectra for the C_9H_{10} isomers *trans*-methylstyrene, α-methylstyrene, and allylbenzene in gas phase and adsorbed at Cu(111) surfaces have been obtained from density functional theory calculations where adsorbate geometries were determined by corresponding total energy optimizations. The three species show characteristic differences in widths and peak shapes of the lowest C $1s \rightarrow \pi^*$ transitions which are explained by different coupling of the π-electron system of the C_6 ring with that of the side chain in the molecules as well as by the existence of nonequivalent carbon centers. The adsorbed molecules bind only weakly with the substrate which makes the use of theoretical NEXAFS spectra of the oriented free molecules meaningful for an interpretation of experimental angle-resolved NEXAFS spectra of the adsorbate systems obtained in this work. However, a detailed quantitative account of relative peak intensities requires theoretical angle-resolved NEXAFS spectra of the complete adsorbate systems which have been evaluated within the surface cluster approach. The comparison with experiment yields almost perfect agreement and confirms the reliability of the calculated equilibrium geometries of the adsorbates. This can help to explain observed differences in the catalytic epoxidation of the three molecules on Cu(111) based on purely geometric considerations. © *2006 American Institute of Physics*. [DOI: 10.1063/1.2212398]

I. INTRODUCTION

Near edge x-ray absorption fine structure (NEXAFS) spectroscopy has proven to be a powerful tool for probing important details of the electronic structure of molecules,[1–3] adsorbate systems,[3–5] and solids.[6–8] Details of the electronic excitations characterizing NEXAFS spectra can yield useful information about local binding and charging, coordination, and—for adsorbate systems—about geometric arrangements of the adsorbates at the surface. In addition, the element specific core ionization potentials which characterize excitation energy regions allow systematic studies of individual atoms or groups of atoms in molecular or solid state environments.

In a recent study,[9,10] Lambert and co-workers examined the catalytic epoxidation of three phenylpropene, C_9H_{10}, isomers, *trans*-methylstyrene (TMS), α-methylstyrene (α-MS), and allylbenzene (AB) (see Fig. 1) at the Cu(111) surface using different surface science techniques. They found that copper can serve as an efficient catalyst for the epoxidation of the (allylic hydrogen containing) alkene side chains in the molecules. However, there are substantial differences in the activity between the three isomers where α-MS is most efficient (62% epoxidation yield), TMS much less (10% yield), and AB shows no epoxidation effect at all. This was explained[9,10] by geometric effects due to differences in the positions of the allylic hydrogen and the C=C double bonds of the side chain with respect to the surface. Here the geometric information was derived from experimental angle-resolved carbon K-edge NEXAFS spectra of the Cu(111)−C_9H_{10} adsorbate systems using the standard Stöhr procedure to evaluate tilt angles of the adsorbates.[3]

While the Stöhr analysis[3] may be reliable for planar molecules with well defined π-electron systems its applicability for more complex molecules with nonplanar components seems somewhat doubtful. An example is the above mentioned allylbenzene whose phenyl and vinyl π-electron systems refer to different symmetry planes. As a result, the molecule does not exhibit a global π symmetry plane which violates a basic assumption of the Stöhr analysis. This makes a Stöhr analysis of the adsorbate geometry for Cu(111)–AB, based on angle-resolved NEXAFS spectra, questionable. For a more detailed analysis of the measured NEXAFS spectra and its geometric origins theoretical studies are essential. In particular, energetic peak splitting and differences in peak shapes observed by experiment can only be explained satisfactorily if theoretical core excitation data and corresponding electronic final states for optimized adsorbate geometries are considered.[11–16]

In this study we present theoretical NEXAFS spectra obtained from density functional theory (DFT) cluster stud-

---
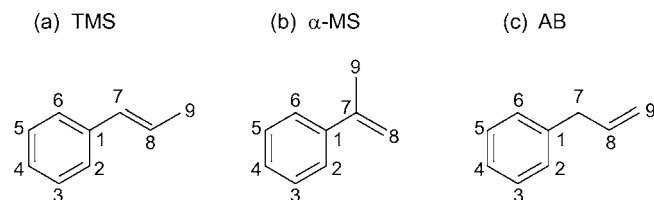[a)]Electronic mail: kolczew@fhi-berlin.mpg.de.

(a) TMS   (b) α-MS   (c) AB

FIG. 1. Structural sketches of (a) *trans*-methylstyrene (TMS), (b) α-methylstyrene (α-MS), and (c) allylbenzene (AB). The atom labeling i of the different carbon centers Ci is used in the interpretation of the NEXAFS spectra and for the geometry discussion.

ies for the three phenylpropenes isomers, both in the gas phase and adsorbed at the Cu(111) surface, together with measured angle-resolved NEXAFS spectra for the Cu(111)−C$_9$H$_{10}$ adsorbate systems. The comparison between theory and experiment yields excellent agreement for all three adsorbate systems, thus, resulting in a reliable description of corresponding adsorbate geometries. This confirms the simple geometric explanation of the different epoxidation yields of the three species found by experiment.[9] In Sec. II we describe our theoretical methods while Sec. III discusses the experimental setup. Sec. IV presents our results and discussion and Sec. V summarizes our conclusions.

II. COMPUTATIONAL DETAILS

The electronic ground states of the three phenylpropene, C$_9$H$_{10}$, isomers under consideration (see Fig. 1) as well as corresponding carbon core electron excitations, yielding theoretical NEXAFS spectra of the free molecules, are obtained from quantum chemical calculations. Here we apply DFT together with the gradient-corrected revised Perdew-Burke-Ernzerhof (RPBE) exchange/correlation functional[17,18] as implemented in the STOBE computer code.[19] This code is based on linear combinations of atomic Gaussian basis sets where we use all-electron triple-zeta valence plus polarization (TZVP) sets in a $[4s,3p]$ contraction with one added d function for carbon[20] and a primitive $(5s)$ set augmented with one p function and contracted to $[3s,1p]$ for hydrogen.[21] The equilibrium geometries of the three molecules are calculated and used to evaluate theoretical NEXAFS spectra of C $1s$ core excitations originating at all nonequivalent carbon centers of the molecules. The complete excitation spectrum $I_{tot}(E)$ of each molecule is determined by electronic dipole transitions with the probability of each excitation (of excitation energy E_n) being given by

$$I(E_n) = 4/3 \pi \chi E_n[m_x^2 + m_y^2 + m_z^2], \qquad (1)$$

where χ is a global scaling factor and the dipole transition matrix element vector

$$m = (m_x, m_y, m_z) = \langle \varphi_i | e \cdot r | \varphi_i \rangle \qquad (2)$$

involves initial C $1s$ core orbitals φ_i and final excited state orbitals φ_f. Here the orbitals are obtained following Slater's transition state (TS) approach[22,23] where in the electronic structure calculations the orbital basis set at the corresponding ionization center is of all-electron individual gauge for localized orbitals (IGLO)-III quality[24] yielding an improved representation of relaxation effects in the inner atomic shells.

TABLE I. Calculated ionization potentials [transition state (TS) and ΔSCF values] of nonequivalent carbon atoms of *trans*-methylstyrene (TMS), α-methylstyrene (α-MS), and allylbenzene (AB). The atom labels are given in Fig. 1. All energies are in eV.

Atom	TMS TS/ΔSCF	α-MS TS/ΔSCF	AB TS/ΔSCF
C1	291.43/289.98	291.43/289.99	291.35/289.90
C2	290.93/289.49	291.05/289.60	291.10/289.66
C3	291.10/289.67	291.18/289.75	291.20/289.76
C4	290.92/289.48	291.05/289.62	291.11/289.69
C5	291.11/289.68	291.18/289.75	291.19/289.76
C6	290.94/289.50	291.05/289.61	291.09/289.65
C7	291.21/289.76	291.71/290.25	291.81/290.38
C8	290.96/289.49	290.61/289.16	291.59/290.12
C9	291.70/290.29	291.67/290.28	291.13/289.67

For the remaining carbon centers effective core potentials[25] (ECPs) describing the C $1s$ core and appropriate valence basis sets are applied. (The use of ECPs simplifies the identification of the core hole orbital while it has only negligible effects on the computed excitation spectrum; see Ref. 26). In addition, a large diffuse even-tempered $[19s,19p,19d]$ basis set,[27] located at the excited carbon center, is included for a more accurate calculation of transition moments and excitation energies yielding an improved description of Rydberg and continuum states (double basis set technique[27]).

The DFT TS approach assumes a frozen molecular ion density and thus neglects electronic relaxation on the molecular ion core upon adding the excited electron. This relaxation is accounted for in an approximate way by shifting all excitation energies by the difference of the ionization potential evaluated with the TS method and the corresponding value from Δ Kohn-Sham self-consistent-field (ΔSCF) calculations; see Table I. Furthermore the excitation spectrum is corrected by a rigid shift of 0.2 eV to higher energies to account for relativistic effects contributing to core excitation[28] [the shift has been recently revised to a surprisingly small value of 0.08 eV (Ref. 29)]. The improved discrete excitation spectrum

$$I_{tot}(E) = \sum_n I(E_n)\delta(E - E_n) \qquad (3)$$

is then subject to a Gaussian convolution with an energy-dependent broadening $\Delta(E)$ to arrive at a theoretical spectrum

$$I_{tot}(E) = \sum_n I(E_n)g(E - E_n, \Delta(E)) \qquad (3a)$$

to be compared with NEXAFS experiments. In the energy region below ionization threshold the broadening $\Delta(E)$ [full width at half maximum (FWHM)] is set to 0.5 eV while a linear increase up to a width of 4.5 eV is assumed for higher energies, as is common practice in the analysis of experimental NEXAFS spectra.[12] The theoretical NEXAFS spectra based on excitation probabilities (1) are appropriate for determining angle-integrated spectra to be compared with experimental spectra of the free molecules. They can also be
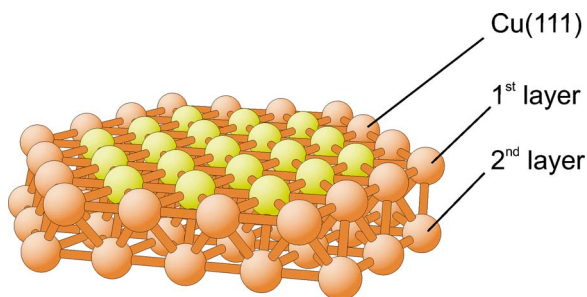
FIG. 2. (Color online) Two-layer Cu(111) substrate cluster, $Cu_{73}(37,36)$, consisting of 73 copper atoms, 37 in the first and 36 in the second layer. Light balls denote atoms described by all electron basis sets while darker balls refer to atoms where effective core potentials together with appropiate valence basis sets are used; see text.

used in assigning experimental absorption peaks to transitions involving specific final state orbitals.

In a second part of this study the three phenylpropenes molecules are considered as adsorbates on the Cu(111) surface where the substrate part of the adsorbate system is simulated by a two-layer $Cu_{73}(37,36)$ cluster of bulk geometry as shown in Fig. 2. The resulting $Cu_{73}C_9H_{10}$ cluster is geometry optimized with respect to all adsorbate atom positions where the substrate atoms are kept fixed at their fcc bulk geometry. In the corresponding electronic structure calculations the 19 surface copper atoms closest to the adsorbate, marked in light gray in Fig. 2, are accounted for by all-electron double-zeta valence plus polarization (DZVP)-type[30] basis sets while for the remaining copper atoms, marked in dark gray in Fig. 2, ECP describing the Cu 1s-3d core together with appropriate $4s,p$ valence bases[31] are used. The $Cu_{73}C_9H_{10}$ clusters with their adsorbates at equilibrium geometry then serve to evaluate theoretical NEXAFS spectra of C 1s core excitations originating at all nonequivalent carbon centers of the adsorbates analogous to the procedure described above for the free molecules. A comparison of the angle-integrated spectra (3a) of the adsorbed molecules with those of the free species can be used to study the overall influence of adsorbate-substrate bonding on spectral features. In addition, theoretical angle-resolved NEXAFS spectra of the adsorbates

$$I_{tot}(E,e) = \sum_n I(E_n,e) \cdot g(E - E_n, \Delta(E)) \qquad (4)$$

for given polarization directions

$$e = (e_x, e_y, e_z) = (\sin\Theta \cos\Phi, \sin\Theta \sin\Phi, \cos\Theta) \qquad (5)$$

of the exciting photons can be calculated according to

$$
\begin{aligned}
I(E_n,e) &= I(E_n,\Theta,\Phi) \\
&= \chi E_n (me)^2 \\
&= \chi E_n (m_x e_x + m_y e_y + m_z e_z)^2 \\
&= \chi E_n \{\sin^2\Theta (m_x \cos\Phi + m_y \sin\Phi)^2 + \cos^2\Theta m_z^2 \\
&\quad + 2\sin\Theta \cos\Theta (m_x \cos\Phi + m_y \sin\Phi) m_z\}, \quad (6)
\end{aligned}
$$

where the Cartesian coordinates system refers to the substrate surface with the z axis pointing perpendicular to the surface plane. The Cu(111) substrate surface exhibits a threefold rotational axis which gives rise to three different adsor-

bate domains which are rotated by 120° with respect to each other. As a consequence, angle-resolved NEXAFS spectra to be compared with experiment have to be summed over all three domains accounted for by polarization vectors e, e', and e'' whose azimuthal angles differ by 120°. Therefore, the $I(E_n,e)$ in (4) have to be replaced by summed transition probabilities[32]

$$
\begin{aligned}
I_{sum}(E_n,e) &= I(E_n,e) + I(E_n,e') + I(E_n,e'') \\
&= I_{sum}(E_n,\Theta) \\
&= \chi E_n \left\{ \left(\frac{1}{2}\right)[m_x^2 + m_y^2]\sin^2\Theta + m_z^2 \cos^2\Theta \right\},
\end{aligned}
$$
$$(7)$$

which depend only on the polar angle Θ of the polarization vector with respect to the surface normal. Assuming the photon polarization to lie in planes perpendicular to the surface—a geometry used in all NEXAFS measurements of the present study—relation (7) can be rewritten as

$$
\begin{aligned}
I_{sum}(E_n,e) &= I_{sum}(E_n,\alpha) \\
&= \chi E_n \left\{ \left(\frac{1}{2}\right)[m_x^2 + m_y^2]\cos^2\alpha + m_z^2 \sin^2\alpha \right\},
\end{aligned}
$$
$$(7a)$$

where α denotes the angle of the incident photon beam with respect to the surface normal. Obviously, the domain superposition leads to a total NEXAFS spectrum determined by

$$I_{tot}(E,e) = \sum_n I_{sum}(E_n,e)g(E - E_n\Delta(E)). \qquad (4')$$

III. EXPERIMENTAL DETAILS

C K-edge NEXAFS measurements were carried out on the SuperESCA beamline at the ELETTRA synchrotron radiation source in Trieste, Italy. The degree of linear polarization of the photons was 0.99 and the photon energy was calibrated (±0.2 eV) by the position of C K-edge dip in the monochromator output. NEXAFS spectra were collected using a double pass 32-channel hemispherical electron analyzer. The angle between the entrance lens of the analyzer and the incoming photon beam was 70° in the horizontal plane. Before each experiment the Cu(111) sample was cleaned by Ar$^+$ sputtering and annealed to 800 K, surface order and cleanliness were checked by low energy electron diffraction (LEED) and x-ray photoemission spectroscopy (XPS), respectively. Reagent grade TMS, α-MS, and AB were outgassed by means of five freeze-pump-thaw cycles and were delivered to the sample via a tube doser. No beam-induced decomposition of the adsorbed layer was observed during these experiments.

IV. RESULTS AND DISCUSSION

A. Phenylpropenes in gas phase, angle-integrated NEXAFS spectra

A full analysis of the equilibrium geometries of the three phenylpropenes, including all bond distances and angles as

TABLE II. Theoretical equilibrium geometries of *trans*-methylstyrene (TMS), α-methylstyrene (α-MS), and allylbenzene (AB) adsorbed on the Cu(111) surface modelled by a $Cu_{73}(37, 36)$ cluster; see text. $\angle$ (A-B-C-D) denotes dihedral angles between atom planes spanned by ABC and BCD. Corresponding values from the free molecule optimizations are added in parentheses. Furthermore, z_{avg} refers to the average distance of the C_6 ring of the adsorbate with respect to the Cu surface plane. In addition, z_{C-Cu} denotes the smallest distance of an adsorbate C center with respect to the Cu surface plane where the number in square brackets gives the corresponding center label; see Fig. 1. Finally, $z_{C=C-Cu}$ refers to the distance of the C=C double bond of the corresponding side chain from the Cu surface; see text. All distances are given in angstroms, angles in degrees.

	TMS	α-MS	AB
$\angle$(C6-C1-C7-C8)	8.7 (4.5)	11.8 (28.6)	95.0 (94.8)
$\angle$(C6-C1-C7-C9)	$\cdots$	11.4 (28.0)	$\cdots$
$\angle$(C1-C7-C8-C9)	177.4(179.2)	$\cdots$	116.3 (120.6)
z_{avg}	3.42	3.40	3.40
z_{C-Cu}	3.42[1]	3.32[8]	3.38[4]
$z_{C=C-Cu}$	3.62	3.43	5.24

well as the Cartesian coordinates, is given in the supplementary information in EPAPS.[33] These molecular geometries are used to calculate C 1s core ionization potentials (IP) of the different molecular carbon centers (using both the TS and ΔSCF methods mentioned above) as well as corresponding angle-integrated C 1s core excitation spectra. An analysis of these spectra based on the character of corresponding excited state orbitals can help to analyze details of the electronic structure and excitations of the phenylpropenes. Unfortunately, no experimental NEXAFS data that would allow comparison with the present calculated spectra seem to be available to date.

TMS is found to equilibrate in its ground state as an almost planar molecule with its C_3H_5 side chain rotated by only 5° out the plane of the C_6 ring; cf. Table II and Ref. 33. As a result, the π-electron systems of the phenyl and allyl components couple to form a common delocalized π-electron system of the molecule. Table I shows C 1s IP values of all carbon centers of the three phenylpropene isomers, evaluated both within the TS and the ΔSCF scheme. While the IP absolute values differ on the average by 1.5 eV between the two approaches the relative IP values show identical trends. For TMS all C 1s IP values are fairly close, differing by 0.5 eV, except for that of C9 which is larger by 0.3 eV. This can be explained by the geometric environment of the C9 atom, see Fig. 1(a), which reflects sp^3-hybridized binding with three hydrogen atoms and does not contribute to the molecular π-electron system.

The calculated total angle-integrated C 1s NEXAFS spectrum of TMS is shown in Fig. 3(a) together with atom-resolved contributions. The spectrum is dominated by a broad asymmetric peak A assigned to transitions of C 1s electrons to the first and second unoccupied π^* orbitals of the molecule as indicated by the plots of the final state orbitals included in Fig. 3(a). Obviously, transitions originating at side chain C centers can be distinguished from those at the ring centers. Here the C $1s \rightarrow \pi^*$ transition referring to C8 is the lowest in energy followed by the corresponding transition at C7 while the C $1s \rightarrow \pi^*$ excitation energies of the other
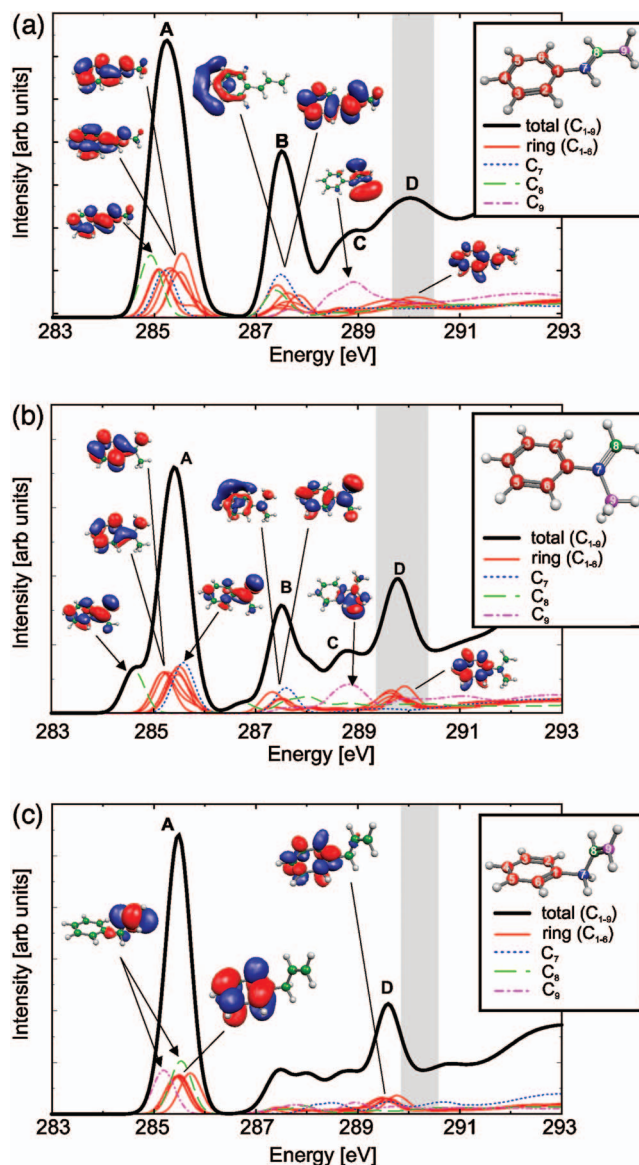

FIG. 3. (Color) Theoretical angle-integrated NEXAFS spectra of gas phase (a) TMS, (b) α-MS, and (c) AB. The total spectra (thick black lines) are shown together with their atom-resolved contributions (thin color lines). The assignment of color lines to carbon centers as well as atom labels are shown in the insets. The gray regions indicate ranges of 1s ionization potentials of nonequivalent carbon atoms. Final state orbitals of the most prominent transitions are included as isosurface plots (positive/negative valued surface parts in blue/red). Arrows indicate final state orbitals corresponding to excitations at a single carbon atom while solid lines indicate examples of similar final state orbitals for a group of carbon atoms. All spectra include relaxation and relativistc effects; see text.

carbon centers are somewhat larger. Altogether, the C $1s \rightarrow \pi^*$ excitation energies are distributed over an energy region of about 0.8 eV. This may be compared with the result for benzene where, for symmetry reasons the corresponding C $1s \rightarrow \pi^*$ excitations are energetically degenerate and C $1s \rightarrow 2\pi^*$ excitations are dipole forbidden.[14] The next prominent peak B in Fig. 3(a) is, for all carbon centers, assigned to transitions from C 1s to the third unoccupied π^* level of TMS as well as to a final state orbital consisting of σ(C–C) bonding and σ(C–H) antibonding character with some Rydberg admixture. This orbital is very similar to final state orbitals of mixed valence/Rydberg character found in previous

TABLE III. Charging of all carbon atoms of α-methylstyrene (α-MS) obtained from Mulliken population analyses. The values refer to results from calculations for the neutral ground state.

Atom	Charge
C1	0.114
C2	−0.229
C3	−0.184
C4	−0.160
C5	−0.184
C6	−0.237
C7	0.135
C8	−0.424
C9	−0.476

studies[14,15] for benzene and other C_6 ring containing molecules. Peak C in Fig. 3(a) is caused by core excitations originating at carbon center C9 located at the end of the side chain; see inset of Fig. 3(a) where the corresponding final state orbital is also of mixed valence/Rydberg character. Finally, peak D close to the ionization threshold [indicated by the gray shaded region in Fig. 3(a)] is assigned to transitions from C 1s to the fourth π^* orbital of TMS.

The α-methylstyrene (α-MS) molecule in its ground state is nonplanar where its C_3H_5 side chain is rotated by 30° out the C_6 ring plane; cf. Table II and Ref. 33. However, the π-electron systems of the phenyl and allyl components still interact reasonably well to form a common delocalized π-electron system of the molecule while the influence of the α-methyl group on the π system can be almost neglected. The C 1s IP values of all carbon centers of the C_6 ring of α-MS, computed both within the TS and ΔSCF scheme (see Table I), are quite similar and differ by only 0.4 eV. In contrast, the IP value for C8, whose electronic structure is also characterized by sp^2 hybridization, is smaller by about 0.5 eV. This IP decrease can be understood by initial state contributions as a result of additional negative charging at the C8 atom due to its two hydrogen neighbors compared to only one for each of the C_6 ring carbons. This becomes evident from the Mulliken atom charges given in Table III. The negative charge is largest at the C9 center while its core IP value is also largest (see Table I). This is, as for TMS, due to its geometric environment which reflects sp^3-hybridized binding with three hydrogen atoms.

The calculated total angle-integrated C 1s NEXAFS spectrum of α-MS is shown in Fig. 3(b) together with atom-resolved contributions. The overall shape of this spectrum is quite similar to that for TMS given in Fig. 3(a). It is dominated by a broad peak A with a low energy shoulder where the main peak is attributed to transitions of C 1s to π^* orbitals of α-MS [cf. final state orbitals plots included in Fig. 3(b)] originating at carbon centers of the C_6 ring and from C7. The low energy shoulder of peak A is assigned to C 1s $\rightarrow \pi^*$ transitions referring to C8 where the energy difference of about 1 eV between the transition from C8 and those from the C_6 ring carbons can be explained as an electrostatic shift due to the increased negative charge at C8 discussed above. Peaks B–D in Fig. 3(b) can be characterized by transitions from C 1s to higher unoccupied levels of α-MS described by

final state orbitals of mixed valence/Rydberg character in complete analogy to those discussed above for TMS.

AB is, in its ground state, also nonplanar with its C_3H_5 side chain rotated by 95° out the C_6 ring plane; cf. Table II and Ref. 33 In addition, the dihedral angle $\angle(C_1\text{-}C_7\text{-}C_8\text{-}C_9)$ of the ground state equilibrium amounts to 120° from the present calculations. Other theoretical studies on AB[34,35] find this angle to be 120° or 0°, depending on basis set size and treatment of correlation in the calculations. However, this discrepancy does not affect the present discussion since the spectra for both geometries show only negligible differences. Therefore we used the equilibrium geometry with a dihedral angle $\angle(C_1\text{-}C_7\text{-}C_8\text{-}C_9)$ of 120°. It suggests an electronic structure where the π-electron systems of the phenyl and allyl components are separate in the molecule and do not couple. As for the two previous molecules, the C 1s IP values of the phenyl carbon centers of AB, cf. Table I, differ by very little, about 0.4 eV. The C7 center, whose electronic structure is described by sp^3 hybridization, analogous to the C9 centers of TMS and α-MS assumes the largest C 1s IP value as discussed above.

The calculated total angle-integrated C 1s NEXAFS spectrum of AB is shown in Fig. 3(c) together with atom-resolved contributions. The shape of this spectrum is somewhat different from those for TMS and α-MS; see Figs. 3(a) and 3(b). There is a dominant peak A near 285.5 eV which is, however, narrower than that in the other two spectra. It is assigned to C 1s $\rightarrow$ lowest π^* transitions originating at carbon centers of the C_6 ring where corresponding final state orbitals are very similar to those of free benzene.[14,15] In addition, peak A contains contributions from C 1s $\rightarrow \pi^*$ transitions assigned to side chain atoms C8 and C9 while core excitations originating at C7 do not contribute. There is an energy region between 287.5 and 289.0 eV without pronounced peaks which collects various C 1s excitations characterized by mixed valence/Rydberg type final state orbitals. Finally, the second dominant peak in the spectrum, denoted D, can be assigned to C 1s transitions originating at carbon centers of the C_6 ring. Here the final state orbital refers to the third unoccupied π^* orbital [located at the C_6 ring, see corresponding orbital plot of Fig. 3(c)] which is quite similar to that of free benzene.[14,15]

A comparison of the most prominent peak A in the angle-integrated NEXAFS spectra of the three phenylpropenes reveals interesting features which are due to differences between the three isomers in their geometry and binding properties. In TMS, which is almost planar, the C_3H_5 side chain couples most strongly with the C_6 ring and the conjugated π-electron systems extends over the whole molecule. As a result, all carbon atoms of the molecule, except for the sp^3-hybridized C9 at the end of the side chain, are chemically similar and core excitations originating from these atoms contribute similarly to peak A within an energy range of 0.8 eV. In α-MS, the electronic coupling of the side chain with the C_6 ring is weakened due to the rotation of the side chain but the π-electron system of the side chain and the ring can still interact and build a perturbed conjugated π system. This results in a low energy peak A due to C1 to C7 core excitations whose width is smaller but comparable with that
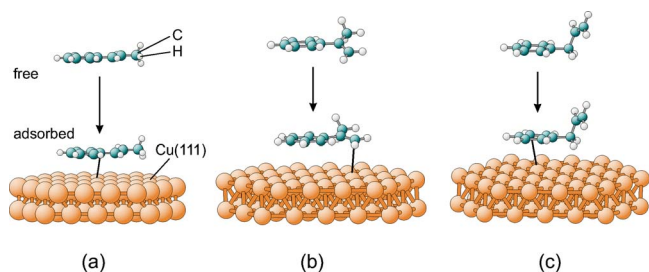
FIG. 4. (Color online) Visual comparison of the theoretical equilibrium geometry of gas phase phenylpropenes with that of the corresponding adsorbate for (a) TMS, (b) α-MS, and (c) AB. In the balls-and-sticks models small light balls denote hydrogen while larger dark balls refer to carbon. The arrows separate the free molecule from the adsorbate where the Cu(111) substrate is shown by the two-layer $Cu_{73}(37,36)$ cluster used in the calculations. In each case the shortest carbon-surface distance is sketched by a gray line.

of TMS. There is an additional shoulder at the low energy side of peak A which is assigned to a shifted C $1s \rightarrow \pi^*$ excitation originating at the C8 atom where the energy shift has been explained as an electrostatic effect. (Interestingly, the NEXAFS spectrum of α-MS in the region of peak A is very similar to that of styrene[15] which differs from α-MS only by replacing the CH_3 group at C9 with hydrogen. The similarity is obvious since the methyl group in α-MS is sp^3-hybridized and does not contribute to excitations referring to peak A.) In AB the electronic coupling between the π-electron systems of the side chain and the C_6 ring is absent for geometric reasons. Thus, the molecule consists of two separate π systems, those of benzene and of propene, with their own characteristic features in the NEXAFS spectrum. The excitation energies of C $1s \rightarrow 1\pi^*$ transitions in benzene and propene are quite similar by accident[36] which explains that the low energy peak A of AB is the most narrow amongst the three isomers.

B. Phenylpropenes adsorbed on Cu(111), geometry and angle-resolved NEXAFS spectra

Table II collects characteristic distances and angles describing equilibrium geometries of the three phenylpropenes adsorbed Cu(111) from the present optimizations where the substrate surface is modeled by the two-layer $Cu_{73}(37,36)$ cluster shown in Fig. 2. In all three cases the geometry parameters of the adsorbate molecules are quite close to those computed for the gas phase equivalents; cf. Table II and EPAPS.[33] This becomes also evident in a visual comparison of the molecules in their gas phase states and as adsorbates shown in Fig. 4. Bond lengths of the molecules are almost unaffected by the interaction with the Cu(111) substrate while bond angles differ somewhat. In particular, the dihedral angles of the ring plane and the side chain in each phenylpropene differ between the gas phase and adsorbed state. For TMS, the dihedral angle $\angle$(C6-C1-C7-C8) increases by 4° due to adsorption rotating the side chain out of the ring plane; see Fig. 4. In contrast, this angle decreases by 17° for α-MS yielding a flatter molecule at the surface where its C=C double bond is bent towards the substrate and the methyl group points away from it. For AB the adsorption leads to only minor distance and angle changes, cf. Table II,

where in the adsorbate geometry the side chain points away from the substrate (see Fig. 4) placing the allylic C=C double bond far away from the surface.

The binding of the three phenylpropenes with the Cu(111) substrate is in all cases quite weak resulting in rather small adsorbate binding energies $E_B = 0.45$ eV for TMS, $= 0.39$ eV for α-MS, $= 0.28$ eV for AB using the gradient-corrected RPBE exchange/ correlation functional.[17,18] This is consistent with rather large values of the average distances between the C_6 rings of the molecules and the surface, $z_{avg} = 3.4$ Å. While the z_{avg} value is very similar for all three adsorbates the surface distance of the carbon atom closest to the surface, z_{C-Cu}, differs somewhat, $z_{C-Cu} = 3.42$ Å for atom C1 of TMS, $= 3.32$ Å for atom C8 of α-MS, $= 3.38$ Å for atom C4 of AB. Another geometric parameter of the adsorbed phenylpropenes, which may be connected with their ability to epoxidize by reacting with surface oxygen, is the distance of the C=C double bonds of the corresponding side chains with respect to the Cu surface, $z_{C=C-Cu}$. This can be quantified by the distance between the bond center (center of gravity of the two carbon atoms involved in the C=C double bond) and the surface. As given in Table II, the present calculations give values $z_{C=C-Cu} = 3.62$ Å for TSM, $= 3.43$ Å for α-MS, $= 5.24$ Å for AB. Thus, oxygen moving along the surface can get closest to the C=C double bond of adsorbed α-MS and react to yield the epoxidized species. The increased distance $z_{C=C-Cu}$ for TMS reduces the epoxidation probability while the rather large $z_{C=C-Cu}$ value for AB makes epoxidation very unlikely to happen. This is consistent with the experimental findings of 62% epoxidation yield for α-MS, 10% for TMS, and no epoxidation for AB discussed previously.[9,10] As an additional geometric effect, which supports the experimental data, we mention the position of allylic hydrogen in the three adsorbates. For adsorbed AB two of its allylic hydrogens get rather close to the Cu surface while the two allylic hydrogens of adsorbed TMS pointing at the surface are further away and adsorbed α-MS offers only one allylic hydrogen near the surface. As a result, oxygen moving along the surface can react most easily with the allylic hydrogen of AB resulting in OH and H_2O surface species and leading to combustion of the adsorbate, a process competing with epoxidation. For adsorbed TMS and α-MS the geometric hydrogen arrangement suggests smaller combustion probabilities, again consistent with experiment.[9,10]

The equilibrium geometries obtained from the present cluster optimizations can be used to evaluate C $1s$ core excitations (including dipole transition matrix elements) and ionization originating at the different carbon centers of the adsorbate molecules within the surface cluster approach. This serves then as a basis for calculating theoretical angle-resolved x-ray absorption spectra as described in Sec. II. Since the adsorbate binding of the three phenylpropenes with Cu(111) is found to be rather weak it is quite suggestive to neglect the adsorbate binding altogether in a first approximation. This is achieved by fixing the free molecules without substrate at geometries identical with those of the adsorbed states at the Cu(111) surface and evaluating corresponding angle-resolved x-ray absorption spectra.

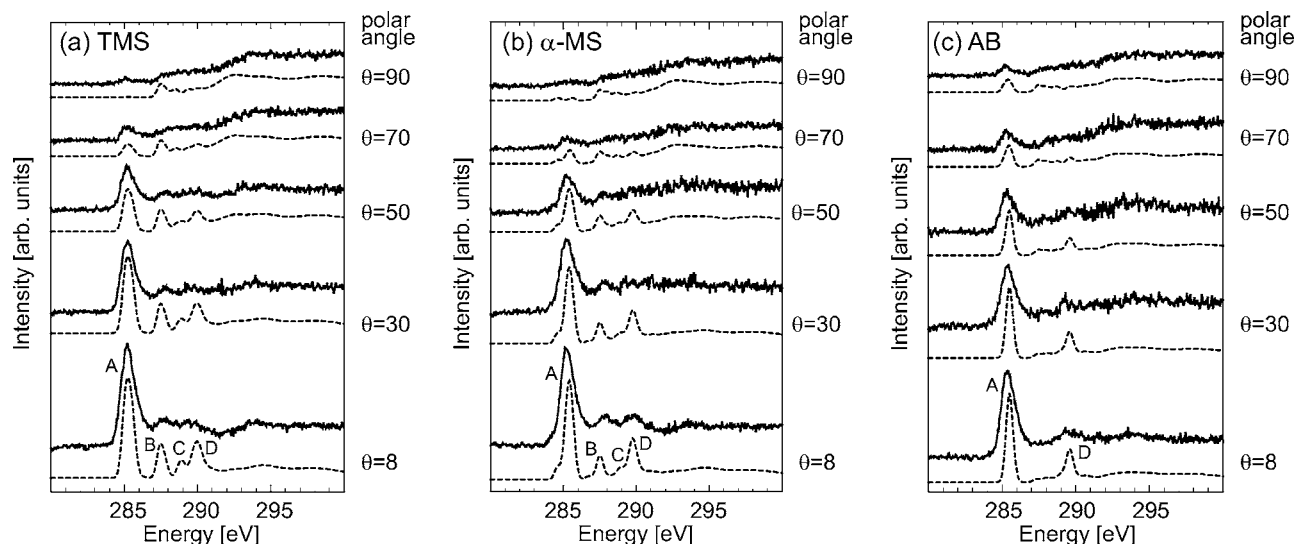Figures 5(a)–5(c) show the theoretical spectra obtained

FIG. 5. Theoretical angle-resolved x-ray absorption spectra of the fixed gas phase phenylpropenes (a) TMS, (b) α-MS, and (c) AB for different angles Θ of the photon polarization vector; see text. Angles Θ are taken with respect to a "surface" normal defined by the normal vectors of the phenyl ring planes. The theoretical spectra (dashed lines) are compared with corresponding experimental monolayer spectra (solid lines) for the adsorbates at Cu(111). All spectra include relaxation and relativistic effects as described in Sec. II.

for the fixed free molecules for different angles Θ of the photon polarization vector calculated according to Eq. (4′) where the experimental NEXAFS spectra of the adsorbate systems are included for comparison. A first inspection of the spectra shows very good agreement between theory and experiment concerning all peak positions in the excitation energy range between 285 and 295 eV. Further more, the theoretical spectra reproduce the experimental angle variations of the different peaks quite accurately. This confirms the overall weak adsorbate-substrate binding found in the total energy calculations of the model systems. However, a more detailed comparison of the theoretical and experimental spectra yields differences in the relative peak intensities which must reflect the influence of adsorbate-substrate interaction. For TMS, see Fig. 5(a), peaks B and D in the theoretical spectrum for $\theta = 8°$ are of almost the same height whereas in the corresponding experimental spectrum the intensity decreases from peak B to peak D. In addition, for $\theta = 8°$ the relative intensity of the main peak A with respect to the higher peaks B through D is smaller by almost a factor two compared with experiment, a discrepancy also found in the spectra of the other polarization angles θ. For α-MS [see Fig. 5(b)], the relative intensity of peak A with respect to the higher energy peaks is also smaller and, in addition, the relative intensities of the higher peaks B and D do not agree between theory and experiment. Finally, for AB [see Fig. 5(c)], the relative intensity of the higher energy peak D is always larger in the theoretical than in the experimental spectra similarly to the other two phenylpropenes.

The rather large relative intensities of the higher energy peaks calculated for the fixed free molecules and compared with the experiment for the adsorbed species can be understood qualitatively. All higher peaks originate from core excitations to quite diffuse final state orbitals. These orbitals are, in particular, for weak adsorbate-substrate coupling, affected more strongly by the presence of the substrate than the localized π-type orbitals of the molecules which contribute

to the intensities of peaks A in the spectra. So the discrepancy between theory and experiment may be explained by quenching effects and should disappear if the complete adsorbate-substrate system is considered. This will be discussed in the following.

Figures 6(a)–6(c) show the theoretical C 1s core excitation spectra computed for the three adsorbed molecules on Cu(111) where the substrate is represented by a two-layer Cu$_{73}$(37,36) cluster. As before, the spectra for different angles Θ of the photon polarization vector are calculated according to Eq. (4′) and compared with the experimental NEXAFS spectra of the adsorbate systems at monolayer coverage. Obviously, the energetic positions of all major peaks as well as corresponding (Θ dependent) relative intensities and peak shapes of the experiments are almost perfectly reproduced by the present calculations. In all cases, the intensities of the higher energy peaks (peaks B–D) are quenched in the adsorbate spectra if compared with those of the fixed free molecules; see Figs. 5(a)–5(c). This is to be expected since, as mentioned above, the adsorbate-substrate interaction affects higher lying diffuse adsorbate orbitals (acting as final excitation orbitals) more strongly than their local π counterparts which determine the intensities of peaks A in the spectra. It should be emphasized that the present theoretical spectra have not been calibrated with experimental NEXAFS data as to the absolute scale of excitation energies. This is reflected in a global spectral energy shift of 0.25 eV between theory and experiment, evidenced in Figs. 6(a)–6(c), which may be due to the choice of the functional. Recently, Takahashi and Pettersson[29] studied the influence of different functionals on calculated excitation energies. For the RPBE exchange and PBE correlation functionals they found an average difference between experiment and theory of −0.44 eV. Our calculated shift of −0.25 eV is clearly in the range of this average value. If the revised relativistic shift of 0.08 eV is applied instead of 0.2 eV used here, the shift
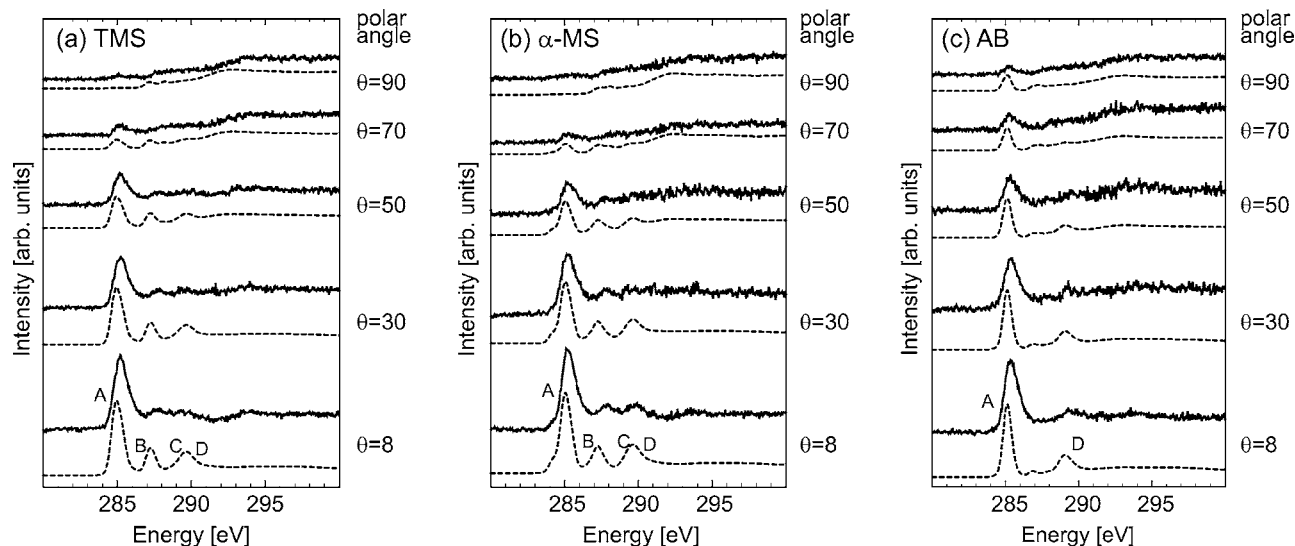
FIG. 6. Theoretical angle-resolved x-ray absorption spectra of the phenylpropenes (a) TMS, (b) α-MS, and (c) AB adsorbed on Cu(111) where the substrate is represented by a two-layer Cu$_{73}$(37,36) cluster. The spectra are shown for different angles Θ of the photon polarization vector with respect to the surface normal. The theoretical spectra (dashed lines) are compared with corresponding experimental monolayer spectra (solid lines). All spectra include relaxation and relativistic effects as described in Sec. II.

between experiment and theory increases to −0.37 eV, which is still in the range of the average value. However, in view of the approximations made in the theoretical treatment this discrepancy is surprisingly small.

V. CONCLUSIONS

The present surface cluster studies on the adsorption of the three phenylpropene isomers, *trans*-methylstyrene (TMS), α-methylstyrene (α-MS), and allylbenzene (AB), at the Cu(111) surface together with theoretical and experimental C 1*s* NEXAFS spectra for these systems provide a clear understanding of the electronic properties of the adsorbates. The theoretical (angle-integrated) gas phase spectra of the three phenylpropenes, Figs. 3(a)–3(c), show sizable differences which can be explained by the molecule-dependent interaction of the propene side chain with the phenyl ring and the location of the propene double bond. This is of particular importance for the shape and width of the low-energy peak structure A assigned to C 1$s \rightarrow \pi^*$ transitions originating at the nonequivalent carbon centers. For TMS the main peak A is broad and asymmetric at its low-energy side while for α-MS there is an additional pronounced low energy shoulder. Peak A in the calculated NEXAFS spectrum is the narrowest for AB. Further more, there are discrepancies between the three molecules concerning their higher-lying peak structures in the spectra due to differences in their diffuse molecular orbital structures. However, a more detailed analysis has to wait until experimental NEXAFS data of the gas-phase phenylpropenes become available.

The calculated equilibrium geometries and electronic properties of the three phenylpropenes adsorbed on the Cu(111) surface [modeled by a two-layer Cu$_{73}$(37,36) substrate cluster] suggest rather weak adsorbate-substrate binding (adsorption energies of only about 0.4 eV) and only very minor geometry changes due to adsorption are found inside the molecules. Therefore, theoretical C 1*s* core excitation

spectra obtained for the free molecules fixed at their corresponding adsorbate geometries and with different angles Θ of the photon polarization vector can give a very satisfactory account of corresponding experimental angle-resolved NEXAFS spectra. In particular, the atom-resolved theoretical analysis of the different spectral features allows a detailed interpretation of the experimental NEXAFS spectra. The agreement between the theoretical and experimental spectra becomes almost perfect if the electronic structure of the full adsorbate systems is considered in the calculations. Both energy positions and relative peak intensities in the experimental spectra are reproduced by theory except for a small global shift of 0.25 eV to lower energies in the theoretical spectra which remains unexplained at present.

The almost perfect agreement between the present theoretical and experimental angle-resolved NEXAFS spectra gives strong indications that the adsorbate geometries of the three phenylpropenes on Cu(111) are quite reliable. Therefore, they can be used to explain observed differences between these adsorbates concerning their catalytic epoxidation behavior using simple geometric considerations as discussed previously.[10] This is of particular importance since a direct experimental determination of the adsorbate geometry based on a standard Stöhr analysis[3] of the angle-resolved NEXAFS spectra is bound to fail for nonplanar hydrocarbon adsorbates, like the phenylpropenes, as pointed out earlier.[3]

[1] R. Püttner, M. Domke, and G. Kaindl, Phys. Rev. A **57**, 297 (1998).
[2] V. Carravetta, G. Polzonetti, G. Iucci, M. V. Russo, G. Paolucci, and M. Barnaba, Chem. Phys. Lett. **288**, 37 (1998).
[3] J. Stöhr, *NEXAFS Spectroscopy*, in Springer Series in Surface Science Vol 25, edited by G. Ertl, R. Gomer, and D. L. Mills (Springer, Heidelberg, 1996).
[4] M. Neuber, M. Zharnikov, J. Walz, and M. Grunze, Surf. Rev. Lett. **6**, 53

(1999).

[5] K. Weiss, S. Gebert, M. Wühn, H. Wadepohl, and C. Wöll, J. Vac. Sci. Technol. A **16**, 1017 (1998).

[6] D. Menzel, G. Rocker, H. P. Steinrück, D. Coulman, P. A. Heimann, W. Huber, P. Zebisch, and D. R. Lloyd, J. Chem. Phys. **96**, 1724 (1992).

[7] T. Okajima, K. Teramoto, R. Mitsumoto, H. Oji, Y. Yamamoto, I. Mori, H. Ishii, Y. Ouchi, and K. Seki, J. Phys. Chem. A **102**, 7093 (1998).

[8] J. G. Chen, Surf. Sci. Rep. **30**, 5 (1997).

[9] R. L. Cropley, F. J. Williams, O. P. H. Vaughan, A. J. Urquhart, M. S. Tikhov, and R. M. Lambert, Surf. Sci. **578**, L85 (2005).

[10] F. J. Williams, R. L. Cropley, O. P. H. Vaughan, A. J. Urquhart, M. S. Tikhov, C. Kolczewski, K. Hermann, and R. M. Lambert, J. Am. Chem. Soc. **127**, 17007 (2005).

[11] M. Nyberg, J. Hasselstrom, O. Karis, N. Wassdahl, M. Weinelt, A. Nilsson, and L. G. M. Pettersson, J. Chem. Phys. **112**, 5420 (2000).

[12] C. Kolczewski, R. Püttner, O. Plashkevych et al., J. Chem. Phys. **115**, 6426 (2001).

[13] L. G. M. Pettersson, H. Ågren, Y. Luo, and L. Triguero, Surf. Sci. **408**, 1 (1998).

[14] R. Püttner, C. Kolczewski, M. Martins, A. S. Schlachter, G. Snell, M. Sant'Anna, J. Viefhaus, K. Hermann, and G. Kaindl, Chem. Phys. Lett. **393**, 361 (2004).

[15] C. Kolczewski, R. Püttner, M. Martins, A. S. Schlachter, G. Snell, M. Sant'Anna, K. Hermann, and G. Kaindl, J. Chem. Phys. **124**, 034302 (2006).

[16] G. Iucci, V. Carravetta, P. Altamura, M. V. Russo, G. Paolucci, A. Goldoni, and G. Polzonetti, Chem. Phys. **302**, 43 (2004).

[17] J. P. Perdew, K. Burke, and M. Ernzerhof, Phys. Rev. Lett. **77**, 3865 (1996).

[18] B. Hammer, L. B. Hansen, and J. K. Norskov, Phys. Rev. B **59**, 7413 (1999).

[19] The program package STOBE is a modified version of the DFT-LCGTO program package DEMON, originally developed by A. St.-Amant and D. Salahub (University of Montreal), with extensions by K. Hermann and L. G. M. Pettersson.

[20] T. H. Dunning, J. Chem. Phys. **55**, 716 (1971).

[21] S. Huzinaga, J. Chem. Phys. **42**, 1293 (1965).

[22] J. C. Slater, in Advances in Quantum Chemistry, edited by P. O. Loewdin (Academic, New York, 1972), Vol. 6, p. 1.

[23] J. C. Slater and K. H. Johnson, Phys. Rev. B **5**, 844 (1972).

[24] NMR-Basic Priniciples and Progress, edited by W. Kutzelnigg, U. Fleischer, and M. Schindler (Springer, Heidelberg, 1990).

[25] A. Mattsson, I. Panas, P. Siegbahn, U. Wahlgren, and H. Åkeby, Phys. Rev. B **36**, 7389 (1987).

[26] L. G. M. Pettersson, U. Wahlgren, and O. Gropen, Chem. Phys. **80**, 7 (1983).

[27] H. Ågren, V. Carravetta, O. Vahtras, and L. G. M. Pettersson, Theor. Chem. Acc. **97**, 14 (1997).

[28] L. Triguero, O. Plashkevych, L. G. M. Pettersson, and H. Agren, J. Electron Spectrosc. Relat. Phenom. **104**, 195 (1999).

[29] O. Takahashi and L. G. M. Pettersson, J. Chem. Phys. **121**, 10339 (2004).

[30] N. Godbout, D. R. Salahub, J. Andzelm, and E. Wimmer, Can. J. Chem. **70**, 560 (1992).

[31] A. Mattson, I. Panas, P. Siegbahn, U. Wahlgren, and H. Åkeby, Phys. Rev. B **36**, 7389 (1987).

[32] C. Kolczewski and K. Hermann, Surf. Sci. **552**, 98 (2004).

[33] See EPAPS Document No.E-JCPSA6-125-706625 for full equilibrium geometries including bond distances, angles, and Cartesian coordinates for all isomers in the gas phase and adsorbed on the Cu(111) surface modeled by a $Cu_{73}(37,36)$ cluster. This document can be reached via a direct link in the online article's HTML reference section or via the EPAPS homepage (http://www.aip.org/pubservs/epaps.html).

[34] S. S. Panja and T. Chakraborty, J. Chem. Phys. **118**, 6200 (2003).

[35] P. J. Breen, E. R. Bernstein, J. I. Seeman, and H. V. Secor, J. Phys. Chem. **93**, 6731 (1989).

[36] A. P. Hitchcock and D. C. Mancini, Atomic and Molecular Core-Edge Excitation Database, http://xray.uu.se/hypertext/corexdb.html, 1994.